OTC 4285

Measured and Predicted Dynamic Response of a Single Pile Platform to Random Wave Excitation

by Michael F. Cook and J. Kim Vandiver, *Massachusetts Institute of Technology*

ABSTRACT

The dynamic response characteristics of an operational single pile platform are investigated in detail. Wind, wave, and response time histories recorded on the platform in March 1980, form the basis for comparison of predicted and measured dynamic response. In the predictive analysis, the components of the total modal damping are separately computed. These damping components include the steel hysteretic, the wave radiation, the viscous hydrodynamic, and the soils damping. Response in the two fundamental bending modes of the structure are predicted using a technique based on the principle of reciprocity for ocean waves. Good agreement between predicted and measured response levels is attained. Combination of the results of the response prediction method with the results of a dynamic finite element model of the platform leads to a versatile expression for the mean rate of accumulation of fatigue damage. This expression, wave spreading factors, and climatological data are used to estimate a fatigue life for the structure.

INTRODUCTION

The understanding of the dynamic response of deepwater structures is a key element in the prediction of fatigue life. This is particularly true of structures with lightly damped natural vibration modes whose natural periods exceed three seconds. There are very few structures that respond linearly in most sea conditions and have sufficiently simple configurations to allow accurate theoretical predictions of dynamic response in directionally spread random seas. The vertical cylindrical caisson satisfies these conditions.

A complete dynamic analysis of a single caisson structure is described in this paper. The modal damping ratio is predicted by analytic means. A finite element model is used to predict the natural mode shapes and soil behavior. The mean square response of the structure is predicted and compared to field measurements with very good agreement. A fatigue life computation is presented which accounts for variation in directional spreading of the seas.

The caisson has many similarities to other more complex fixed deepwater structures. It has similar mode shapes, natural periods, and damping ratios. The caisson has the same range of Reynolds numbers and Keulegan-Carpenter numbers as large tubular members on jacket structures. It has similar soil behavior. As a consequence the insights gained from an in-depth analysis of this simple structure provide a better understanding of the behavior of much larger and complex but dynamically similar deepwater platforms.

PLATFORM DESCRIPTION

The single pile platform which is the focus of this report is a triple-decked single well gas production platform located in South Marsh Island Block 33 in the Gulf of Mexico. A three dimensional drawing of the platform, which is operated by AMOCO Oil Company, is shown in Figure 1. The caisson stands in 89 feet of water and the pile diameter is four feet at the water line and seven at the mudline. The annulus between the main pile and the drive pile is grouted. The natural periods of the two orthogonal fundamental flexural modes of the structure are almost identical, each with a value of approximately 3.1 seconds. With these natural periods, the platform exhibits significant first mode dynamic response.

In March, 1980, the authors recorded wind, wave and response time histories on the structure for later analysis and comparison with predicted response values. A complete description of the data analysis is contained in Ref. [1]. A total of six reels of data were recorded on three separate days. A summary of the pertinent information derived from the five reels which contained horizontal biaxial accelerometer data is shown in Table 1. The other reel of data, reel 2, had time histories from four accelerometers distributed vertically over the structure but pointing in the same direction. This data was used to estimate mode shapes and is reported in OTC Paper No. 4286 [2]. One of the five remaining data sets, reel 5, included tests of a dynamic absorber. These results are described in OTC Paper No. 4283 [3].

SINGLE-DEGREE-OF-FREEDOM EQUIVALENT MODEL

This single pile platform responds significantly in only its fundamental bending modes. To predict the response in these natural modes, an equivalent, linear, single degree of freedom (SDOF) system was defined for both modes. This technique is applicable for structures which behave linearly and have small damping. The total response is obtained by superposition of the modal responses.

The equation of motion that represents first mode response of the caisson when excited by ocean waves contains terms which depend on the relative acceleration and velocity between the water particles and the generalized coordinates which represent platform motions. For this structure in commonly occurring low to moderate sea states non-linear drag force or velocity dependent excitation is negligible and can be dropped. However, this does not necessarily imply that viscous damping losses can be ignored. These must be evaluated separately.

When the total damping is small, damping can be modelled using an equivalent linear dashpot which equates platform energy losses with the SDOF model energy losses. The SDOF equivalent equation for a mode is of the form

$$M\ddot{q} + (R_{ST} + R_{RAD} + R_{VH} + R_{SOIL})\dot{q} + Kq = F(t) \quad (1)$$

where M = modal virtual mass of the structure (includes added mass)

R_{ST} = modal steel hysteretic damping

R_{RAD} = modal radiation or wave making damping

R_{VH} = modal viscous hydrodynamic damping

R_{SOIL} = modal soils damping

K = modal stiffness of the structure

q = generalized coordinate obtained from modal analysis for the particular mode

$F(t)$ = total linear modal force

The undamped modal natural frequency, ω_n, and damping ratio, ξ_T, are

$$\omega_n = \sqrt{K/M}. \quad \quad \quad \quad \quad \quad \quad \quad \quad \quad (2)$$

$$\xi_T = \frac{R_T}{2\omega_n M} = \frac{R_{ST} + R_{RAD} + R_{VH} + R_{SOIL}}{2\omega_n M}$$

$$= \xi_{ST} + \xi_{RAD} + \xi_{VH} + \xi_{SOIL} \quad \quad (3)$$

Using these, the SDOF equivalent system reduces to

$$\ddot{q} + 2\omega_n \xi_T \dot{q} + \omega_n^2 q = F(t)/M \quad \quad \quad (4)$$

To use this equation to accurately predict response requires knowledge of the total modal damping present within the vibrating system. As suggested in Equation 3, the total modal damping is a combination of four major damping sources. In the next four sections, each source will be identified and an equivalent modal damping ratio will be estimated from theoretical considerations.

DAMPING RATIO PREDICTION

Steel Hysteretic Damping

Steel hysteretic damping refers to the energy lost due to internal dissipation within a steel member under cyclic loading. As discussed in Ref. [1], the fraction of the total strain energy dissipated per cycle due to steel hysteretic damping within the outer pile of the caisson may be approximated by the following:

$$\frac{\Delta V_{ST}}{V_{ST}} = 2JE = 2\pi(.0047) \quad \quad \quad \quad (5)$$

where ΔV_{ST} = strain energy dissipated in the outer pile per cycle

V_{ST} = peak strain energy stored in the outer pile

J = constant = 500×10^{-12}/psi for SAE 1020 steel

E = Youngs modulus = 29.5×10^6 psi for SAE 1020 steel.

The energy loss per cycle can be simply expressed in terms of a linear equivalent damping ratio for a single degree of freedom system. The correct relationship is given by

$$4\pi\xi_{ST} = \frac{\Delta V_{ST}}{V_{ST}} \quad \quad \quad \quad \quad \quad (6)$$

Therefore,

$$\xi_{ST} = \frac{.0047}{2} = 0.24\% \quad \quad \quad \quad \quad (7)$$

This damping ratio is assumed to apply to the other materials in the structure as well; particularly the grout. The grout would probably have somewhat higher losses than this and therefore the value of 0.24% as an overall material hysteretic damping is likely a lower bound. In the remainder of the report this damping will continue to be referred to as ξ_{ST}, in reference to the losses in the steel. However, it is applied to the entire mechanical energy of the structure.

Radiation (Wave Making) Damping

A platform oscillating in the ocean creates waves which radiate outward, dissipating energy away from the structure. For a vertical cylinder of uniform diameter, the modal radiation damping can be estimated using linear potential flow theory. A derivation is contained in a 1976 report by Petrauskas [4].

Based on these results, an approximate expression for the modal radiation damping coefficient for a non-uniform vertical cylinder which creates deepwater radiated waves is

$$R_{RAD}(\omega) = \frac{\pi \rho_w \omega}{e^{2kh} + 4kh} \left[\int_{-h}^{0} d(z) P_1 \left(\frac{kd}{2}\right) \psi(z) e^{k(z+h)} dz \right.$$

$$\left. \int_{-h}^{0} \psi(z) e^{k(z+h)} dz \right] \quad \ldots \ldots \ldots \text{(8)}$$

where z = vertical coordinate, positive upwards from the water line

ρ_w = density of water

ω = frequency of radiated waves

k = wave number

$d(z)$ = cylinder diameter

h = water depth

$\psi(z)$ = mode shape (estimated from finite element model)

$P_1(kd/2) = \frac{\pi}{2} \left(\frac{kd}{2}\right)^3$ for $\frac{kd}{2} < \frac{1}{2}$

Equation 8 was evaluated numerically using the parameters associated with the operational single pile platform in first mode response. The modal radiation damping ratio was found to be

$$\xi_{RAD} = 0.11\% \quad \ldots \ldots \ldots \ldots \ldots \ldots \text{(9)}$$

This result is approximate in the sense that the Petrauskas result is strictly applicable to a cylinder with a uniform diameter. Equation 8 relaxes this constraint to allow for a diameter which changes slowly and then only at a substantial distance below the waterline. As a check on this result, the radiation damping was computed for a cylinder with a constant diameter of four feet. For it $\xi_{RAD} = 0.10\%$.

Viscous Hydrodynamic Damping

Viscous hydrodynamic damping is related to the separated flow drag force term in Morison's equation. An expression for the modal viscous hydrodynamic damping coefficient applicable for first mode response of a vertical cylinder as shown by Dunwoody [5] is

$$R_{VH} = \int_{-h}^{0} \frac{1}{2} \rho_w \, d \, C_D \sqrt{\frac{8}{\pi}} \, \sigma_{\dot{r}}(z) \, \psi^2(z) dz \quad \ldots \ldots \text{(10)}$$

where C_D = drag coefficient

$\sigma_{\dot{r}}$ = r.m.s. relative velocity.

As defined here, R_{VH} is proportional to the relative velocity, which increases with sea state, and can only be obtained by iteration. However, if water particle velocities are assumed to be much larger than structural velocities, $\sigma_{\dot{r}}$ can be approximated by the r.m.s. water particle velocity, σ_u, which can be estimated from Equation 11.

$$\sigma_u^2(z) = \int_{0}^{\infty} 4\pi^2 f^2 \, G_\eta(f) e^{2kz} df \quad \ldots \ldots \ldots \text{(11)}$$

where f = cyclic frequency (Hz)

$G_\eta(f)$ = wave amplitude spectrum

Equation 11 is valid for deep water waves which decay exponentially. Using a Bretschneider (ITTC) [6] two parameter wave spectrum,

$$G_\eta(f) = \frac{1.25}{4} H_s^2 \frac{f_p^4}{f^5} e^{-1.25(f_p/f)^4} \quad \ldots \ldots \text{(12)}$$

where H_s = significant wave height

f_p = peak wave frequency (Hz).

estimates of the modal viscous hydrodynamic damping were obtained for the sea states corresponding to experimentally derived values of H_s and f_p. Typical values of ξ_{VH} in the experiments were in the vicinity of 0.15%. The detailed results will be summarized later. As computed above, the modal viscous hydrodynamic damping is probably an upper bound since a unidirectional wave spectrum has been used to compute σ_u. Spreading would decrease the effective σ_u.

Soils Damping

Compared with the other components of the total damping, the characterization and modelling of soils damping is more complex and less well established. Two types of soil damping exist; material (internal) soil damping, which is a hysteretic form of damping, and geometric (radiation) damping, which is analogous to wave making damping. Material damping is usually specified as the fraction of soil strain energy dissipated per cycle and is expressed as 4π times a constant soils damping ratio, ξ_{smd}, which is believed to have a value between 3 and 10%. ξ_{smd} is also known as the specific damping ratio. Geometric damping is present only if the frequency of oscillation exceeds a threshold value which depends on the soil stratum. In general, geometric damping is not significant for small structures at the frequencies associated with wave loading, in Gulf of Mexico sediments.

As developed in detail in Ref. [1], an equivalent modal soils damping ratio ξ_{SOIL} can be estimated from the soil material damping ratio ξ_{smd} by computing the ratio of the energy loss per cycle in the soil to the total caisson energy. The method utilizes the lumped soil spring foundation of the finite element idealization of the caisson to compute the soil strain energy. The final expression for ξ_{SOIL} is

$$\xi_{SOIL} = \frac{\Delta V_{SOIL}}{4\pi V_T} = \frac{\xi_{smd}}{M\omega_n^2} \sum_{i=1}^{n} K_s(z_i) \psi^2(z_i) \quad \ldots \ldots \text{(13)}$$

where $\Delta V_{SOIL} = 4\pi \xi_{smd} V_{SOIL}$

$$= 4\pi \xi_{smd} \left(\frac{1}{2} \Sigma K_s(z_i) \psi^2(z_i) a_o^2\right)$$

$$V_T = \frac{1}{2} K a_o^2 = \frac{1}{2} M \omega_n^2 a_o^2 = \text{total caisson energy}$$

$K_s(z_i)$ = lumped soil spring stiffness at $z = z_i$

$\psi^2(z_i)$ = value of the mode shape at $z = z_i$

n = number of lumped soil springs used in this finite element model.

Equation 13 was evaluated using the four soil springs of the finite element model of the caisson and the results are shown in Table 2. This technique is approximate and research leading to the development of new techniques is warranted.

TOTAL DAMPING RATIO MEASUREMENTS

The total modal damping was estimated for each of the two fundamental bending modes from biaxial accelerometer data recorded in March 1980. To isolate the fundamental modal directions, a correlation function rotation scheme based on a Mohr's circle algorithm was used. In this analysis, the modal orientation is defined as that orientation for which the time histories from a biaxial pair of accelerometers would have a minimum coherence at the natural frequencies of the two fundamental bending modes. This procedure is described in Ref. [1]. Once the modal orientation is determined, single-channel MEM (Maximum Entropy Method) spectral analysis is used to estimate natural frequencies and damping ratios. The damping ratio estimate is based on the half-power bandwidth method [7].

The results of the damping estimation are shown in Table 2 for three different days of testing. In this table, items 2, 3, 4, 6, and 7 were theoretically obtained, as previously described; item 1 is an experimental value. The error bounds on the measured total damping ratio are 95% confidence bounds. The viscous hydrodynamic damping was estimated, assuming a drag coefficient of 1.0 and applying values of H_s and ω_p derived from the measured wave spectra. Row 5 is the soils damping required to make the total experimental damping value equal the total theoretical. The values shown suggest an average value of $\xi_{SOIL} = 0.6\%$, which falls in the expected range of the analytically estimated values.

RESPONSE PREDICTION

After the modal equivalent damping components have been estimated, the next step is to predict modal response. The reciprocity method of response prediction, proposed by Vandiver [8], will be used for this purpose. This approach utilizes the principle of reciprocity for ocean waves which relates the radiation damping of a structure oscillating in a calm sea to the linear wave force exerted on the structure if it were held fixed in incident waves. This technique yields a simple result for the mean square modal response and its use is valid only for lightly damped modes excited by linear wave forces. This method directly incorporates wave spreading effects.

The caisson is an ideal structure to test this modal response prediction technique because the structure is axi-symmetric and the two fundamental bending natural frequencies are almost identical.

To demonstrate the performance of this response prediction method, the coordinate system shown in Figure 2 was used. In this figure, the x and y axes define the orientation of the two fundamental bending modes of the caisson. The angle θ defines the angle between the x-modal direction and the mean wave direction in a directionally spread sea. The terms σ_x^2 and σ_y^2 represent the mean square modal displacement response on the helideck along the x and y modal axes, respectively.

The prediction of the mean square modal response

of the x-mode within two half power bandwidths of the resonant frequency f_x is shown in Equation 14.

$$\sigma_x^2 = \frac{C_x \rho_w g^3}{80\pi^5 M_x f_x^5} \; G_\eta(f_x) \; \frac{\xi_{RAD}(f_x)}{\xi_T(f_x)} \quad \ldots \ldots \ldots (14)$$

The expression for the y-mode is identical with the x subscripts replaced by y subscripts. The term C_x depends on both structural geometry and the directional wave amplitude spectrum. In this paper, the directional wave amplitude spectrum is modelled using frequency independent spreading functions as defined in the following equation.

$$G_\eta(f,\theta) = G_\eta(f) \; D(\theta) \quad \ldots \ldots \ldots \ldots (15)$$

where $G_\eta(f,\theta)$ = directional wave amplitude spectrum

$\quad\quad D(\theta)$ = spreading function

$\quad\quad\quad \theta$ = angle of incidence of various wave components

When integrated over all possible wave incidence angles, the directional wave amplitude spectrum satisfies

$$G_\eta(f) = \int_0^{2\pi} G_\eta(f,\theta) \; d\theta \quad \ldots \ldots \ldots \ldots (16)$$

For a single pile platform, the expressions from Ref. [8] for C_x and C_y simplify to

$$C_x = 2\int_0^{2\pi} D(\theta) \cos^2\theta d\theta \quad \ldots \ldots \ldots \ldots (17)$$

and

$$C_y = 2\int_0^{2\pi} D(\theta) \sin^2\theta d\theta \quad \ldots \ldots \ldots \ldots (18)$$

The sum of Equations 17 and 18 is trivial to evaluate, because $\sin^2\theta$ plus $\cos^2\theta$ yields 1.0 and the integral

$$\int_0^{2\pi} D(\theta) d\theta = 1.0 \quad \ldots \ldots \ldots \ldots (19)$$

and therefore

$$C_x + C_y = 2.0 \quad \ldots \ldots \ldots \ldots (20)$$

Therefore, even though the actual spreading function is unknown, the total mean square response may be predicted by summing the individual mean square responses σ_x^2 and σ_y^2.

$$\sigma_x^2 + \sigma_y^2 = \frac{\rho_w g^3}{40\pi^5 M_x f_x^5} \; G_\eta(f_x) \; \frac{\xi_{RAD}(f_x)}{\xi_T(f_x)} \quad \ldots (21)$$

where it has been assumed that the natural frequencies, modal masses and damping ratios of both modes are approximately equal. The x subscript has been retained

in Equation 21 to reflect the properties of both modes. It has also been assumed that the responses of the two modes x and y at their common natural frequency are uncorrelated. This has been confirmed in the field experiments. The coherence between the two modal responses is less than 0.05.

The measured data is in terms of acceleration. For purposes of comparing predicted and measured data it is convenient to express Equation 21 in terms of mean square acceleration. The mean square response within a half power bandwidth of the natural frequency is a narrow band random process and the following simple relation may be used for either the x or y directed modes.

$$\sigma_{\ddot{x}}^2 = 16\pi^4 f_x^4 \sigma_x^2 \quad \ldots \ldots \ldots \ldots (22)$$

Therefore, the total mean square acceleration may be expressed as,

$$\sigma_a^2 = \sigma_{\ddot{x}}^2 + \sigma_{\ddot{y}}^2 = \frac{2\rho_w g^3}{5\pi M_x f_x} \; G_\eta(f_x) \; \frac{\xi_{RAD}(f_x)}{\xi_T(f_x)} \quad \ldots \ldots (23)$$

The natural frequency f_x of this platform was measured as well as the total modal damping ξ_T. The modal mass was determined from the finite element model and the radiation damping was computed theoretically. Therefore using measured values of the wave amplitude spectrum evaluated at the natural frequency it is possible to predict the total mean square acceleration response of the structure and compare it to that observed.

The results are summarized in Table 3 for data taken on two separate days. The predicted and measured values are in very close agreement. The actual error in the predictions is substantially less than might have been expected considering the uncertainty in the estimates of the total damping ratio. This is the first known experimental confirmation of the response prediction technique embodied in Equation 14.

DESCRIPTION OF THE FINITE ELEMENT MODEL

In order to estimate both the fundamental flexural mode shape and the relationship between platform dynamics and stresses within the pile, a 21-node two-dimensional dynamic finite element (F.E.) model of the single pile platform was developed. In this model, the platform was represented using 14 beam elements and the soil was replaced by four linear soil springs. A schematic of the F.E. model is shown in Figure 3 and a detailed description of its formulation is contained in Ref. [1]. To achieve model natural periods which closely matched the measured values required iteration of the soil spring stiffnesses.

Both the fundamental flexural mode shape and the soil spring stiffnesses required in the damping estimation were obtained from the optimized F.E. model. In addition, the maximum stress in the pile, when subjected to sinusoidal wave excitation, at the natural frequency was found to be at a level approximately 26 feet below the mudline. For vibration in the fundamental mode, the helicopter deck displacement to maximum stress transfer function was determined to be 4.95 KSI/foot. This value is required later in the prediction of fatigue life.

DYNAMIC RESPONSE FATIGUE LIFE ESTIMATION

For offshore structures experiencing significant dynamic response in low and moderate sea states, the governing design criteria is often the prevention of failure caused by low stress, high cycle fatigue. To estimate the dynamic response fatigue life of the operational single pile platform, the reciprocity method of response prediction and the dynamic finite element model were combined with a fatigue accumulation model which assumes the stress process is a narrow band Gaussian process with Rayleigh distributed peaks. The result is a versatile expression for the mean rate of accumulation of fatigue damage. The details of this procecure are outlined below.

The expression for the mean rate of accumulation of fatigue damage, based on a stress range S-N curve, is from Ref. [9]

$$F_i = \frac{\nu_o^+}{c} (2^3 \sigma_s^2)^{b/2} \; \Gamma(1+b/2) \quad \ldots \ldots \ldots (24)$$

where F_i = mean rate of accumulation of fatigue damage at a location in the structure which experiences a mean square stress σ_s^2

ν_o^+ = average zero upcrossing rate of the stress process

$\Gamma(\ )$ = Gamma function

b, c = constants of the stress range S-N curve.

The dynamic finite element model was used to determine the relationship between the maximum stress in the pile and helideck displacements in mode x. Mathematically, this relationship can be expressed as

$$\sigma_s^2 = B^2 \sigma_x^2 \quad \ldots \ldots \ldots \ldots \ldots \ldots (25)$$

where B = maximum stress/helideck displacement transfer function

B = 4.95 KSI/ft.

A value of σ_x^2 was estimated using the reciprocity method, as defined in Equation 14, in conjunction with the Bretschneider (ITTC) wave spectrum of Equation 12. This technique requires that the wave environment at the location be modelled with a set of significant wave height (H_s) and peak wave period (T_p) pairs, each with an assigned annual probability of occurrence (P_i). The resulting expression for the mean rate of accumulation of dynamic response fatigue damage in mode x due to sea state i is shown in Equation 26.

$$F_i = \frac{f_x}{c} \left[\frac{B^2 \rho_w g^3}{32\pi^5} \; \frac{C_x H_s^2}{M_x} \; \frac{f_p^4}{f_x^{10}} \; \frac{\xi_{RAD}}{\xi_T} \; e^{-1.25\left(\frac{f_p}{f_x}\right)^4} \right]^{b/2}$$

$$\cdot \Gamma(1+b/2) \quad \ldots \ldots \ldots \ldots \ldots \ldots (26)$$

where $\nu_o^+ = f_x$

$f_p = 1/T_p$

In this equation, all the parameters which affect the dynamic response fatigue life of a structure are included in a readily usable form. Finally, a fatigue

life estimate (FLE) can be obtained using

$$FLE = 1 \Big/ \sum_{i=1}^{j} F_i P_i \quad \ldots \ldots \ldots \ldots \ldots (27)$$

where j = total number of sea states.

Fatigue Life Calculation

The fatigue life of the operational single pile platform was estimated using the twelve Gulf of Mexico sea states given in Ref. [10]. For each sea state, Equation 26 was used to compute the rate of accumulation of fatigue damage associated with first mode response of the caisson. The AWS-X modified stress range S-N curve was used to determine values for b and c (b = 4.38, c = 2.64 x 10^{11}). In addition, it was assumed that the modal frequency and modal mass remain constant over the lifetime of the structure. For the initial estimate, the ratio ξ_{RAD}/ξ_T was fixed for all sea states at 0.2. The selection of a representative value of C_x is not straightforward. However, two useful limiting cases may be easily evaluated.

The worst case scenario is one in which over the lifetime of the structure the seas are unidirectional and only excite the x directed mode. In other words, all waves are incident at $\theta=0$. For this case, the response in the y direction must be zero and therefore, from Equation 20, C_x = 2.0.

The least damaging case is one in which the directional spreading is uniform over all angles. The result of this is that both modes must respond equally and therefore, $C_x = C_y = 1.0$.

These two limiting cases will yield upper and lower bound fatigue life estimates for this caisson when substituted into Equations 26 and 27. The result for the uniform spreading case is a fatigue life of 161 years. Unidirectional spreading reduces this estimate to a worst case fatigue life of 35 years. These calculations were computed using a conservative estimate of ξ_{RAD}/ξ_T = 0.2. In fact, the field measurements indicate it is approximately half that value. Accounting for this increases the estimated fatigue life by a factor of approximately four. These results indicate that the fatigue life of this structure is between 140 and 644 years. These predictions do not account for fatigue damage caused by quasi-static response of the structure to large low frequency waves. Though many fewer in number, these waves will reduce the fatigue life somewhat. Non-linear drag exciting forces at the natural frequency of the structure have also been neglected.

Many factors influence fatigue life predictions. Natural frequencies, damping ratios, and wave spreading are particularly important. For a more complete discussion of the sensitivity of fatigue life predictions to these factors the reader is directed to Ref. [11].

CONCLUSIONS

In this paper a complete dynamic analysis of a single caisson platform has been presented. A finite element model provided mode shapes, stress transfer functions and some insight into the behavior of the soil. Predictions of all components of damping were made. Field measurements were used to obtain estimates of natural frequencies, damping ratios and mode shapes (see OTC 4286). The measured mean square response was compared to predictions based on the reciprocity method and found to be quite accurate. Finally, an analysis of the fatigue life of the structure was performed, in such a way that the sensitivity of fatigue calculations to directional spreading of the waves was clearly indicated.

NOMENCLATURE

a_o	modal amplitude
b, c	constants of the stress range S-N curve
B	maximum stress in the pile per foot of helideck displacement
C_D	drag coefficient
C_x, C_y	constants dependent on directional spreading
d	pile diameter
$D(\theta)$	wave spreading function
E	Young's modulus of elasticity
f	cyclic frequency (Hz)
f_p	peak wave frequency
FLE	fatigue life estimate
F(t)	modal wave force on fixed structure
$G_\eta(f)$	wave amplitude spectrum
$G_\eta(f,\theta)$	directional wave amplitude spectrum
h	water depth
H_s	significant wave height
J	constant in steel hysteretic damping expression
k	wave number
K	total modal stiffness
$K_s(z_i)$	soil spring stiffness at $z=z_i$
M	total modal virtual mass
P_i	annual probability of occurrence for sea state i
$P_1(kd/2)$	function defined in [4]
q	modal displacement coordinate
R_{RAD}	modal radiation damping coefficient
R_{ST}	modal steel hysteretic damping coefficient
R_T	total modal damping coefficient

Symbol	Definition
R_{VH}	modal viscous hydrodynamic damping coefficient
T_p	peak wave period
V_{SOIL}	peak strain energy stored in the soil during a cycle
ΔV_{SOIL}	strain energy dissipated in the soil per cycle
V_{ST}	peak strain energy stored in the steel members during a cycle
ΔV_{ST}	strain energy dissipated in the steel members per cycle
V_T	maximum energy stored in the total structure during a cycle
$\Gamma(\ )$	Gamma function
θ	wave incidence angle
θ_0	mean wave direction of directionally spread sea
ν_0^+	zero upcrossing frequency of stress process (Hz)
ξ_{RAD}	modal radiation damping ratio
ξ_{smd}	specific damping ratio of soils
ξ_{SOIL}	modal soils damping ratio
ξ_{ST}	modal steel hysteretic damping ratio
ξ_T	total modal damping ratio
ξ_{VH}	modal viscous hydrodynamic damping ratio
ρ_w	density of water
$\psi(z)$	mode shape ordinate at elevation z
ω_n	undamped modal natural frequency
σ_a^2	total mean square helideck acceleration due to x and y first mode responses
$\sigma_{\dot{r}}$	root mean square relative velocity
σ_x^2, σ_y^2	mean square helideck displacement in x and y modes
$\sigma_{\ddot{x}}^2$, $\sigma_{\ddot{y}}^2$	mean square helideck accelerations in x and y modes

ACKNOWLEDGEMENTS

REFERENCES

1. Cook, M.F., "Damping Estimation, Response Prediction and Fatigue Calculation of an Operational Single Pile Platform," Engineer Thesis, Massachusetts Institute of Technology and Woods Hole Oceanographic Institution, January, 1982.

2. Briggs, M.J. and Vandiver, J.K., "Multichannel Maximum Entropy Method of Spectral Analysis Applied to Offshore Platforms," Proceedings of the 1982 Offshore Technology Conference, Paper No.4286, Houston, Texas, May 1982.

3. Lu, X. and Vandiver, J.K., "Damping and Natural Frequency Estimation Using the Least Pth Optimization Technique," Proceedings of the 1982 Offshore Technology Conference, Paper No. 4283, Houston, Texas, May, 1982.

4. Petrauskas, C., "Hydrodynamic Damping and 'Added Mass' for Flexible Offshore Platforms," U.S. Army Coastal Engineering Research Center, Report CERC-TP-76-18, October, 1976.

5. Dunwoody, A.B. and Vandiver, J.K., "The Influence of Separated Flow on the Dynamic Response of Offshore Structures to Random Waves," Proceedings of the Hydrodynamics In Ocean Engineering Conference, Trondheim, Norway, August 1981.

6. Connor, J.J. and Sunder, S.S., "Wave Theories, Wave Statistics and Hydrodynamic Loads," Department of Civil Engineering, Massachusetts Institute of Technology, January, 1980.

7. Campbell, R.B., and Vandiver, J.K., "The Estimation of Natural Frequencies and Damping Ratios of Offshore Structures", Proceedings of the 1980 Offshore Technology Conference, Paper No. 3861, Houston, Texas, May 1980.

8. Vandiver, J.K., "Prediction of the Damping Controlled Response of Offshore Structures to Random Excitation," Society of Petroleum Engineers Journal February 1980.

9. Crandall, S.H., Mark, W.D., Random Vibration in Mechanical Systems, Academic Press, New York, 1963.

10. Kinra, R.K., Marshall, P.W., "Fatigue Analysis of the Cognac Platform", Proceedings of the 1979 Offshore Technology Conference, Paper No. 3378, Houston, Texas, May, 1979.

11. Vandiver, J.K., "The Sensitivity of Fatigue Life Estimates to Variations in Structural Natural Periods, Modal Damping Ratios, and Directional Spreading of the Seas," Proceedings of the Third International Conference on the Behavior of Offshore Structures, M.I.T., 1982.

TABLE 1

SUMMARY OF WAVE, WIND AND RESPONSE DATA

	REEL #1	REEL #3	REEL #4	*REEL #5	REEL #6
Date	3/24/80	3/25/80	3/28/80	3/28/80	3/28/80
Time	1510 - 1630	1215 - 1335	1050 - 1210	1510 - 1615	1630 - 1715
Observed Wave Height (ft)	NW 1-3	ENE 5-8	ENE 2-4	ESE 3-5	ESE 3-5
Observed Wind Speed (knots)	NW @ 20	ENE @ 30	ENE @ 10	ESE @ 20	ESE @ 20
Peak Wave Period (sec)	-	7.28	6.79	7.10	7.10
Significant Wave Height (ft)	-	4.12	3.32	3.59	3.80
Orientation of Mode x	25°S of E	13°N of E	35°N of E	7°S of E	15°S of E
Mode x Natural Frequency Est. (Hz)	.325	.323	.323	.323	.324
x Mode Total Damping Ratio Est.	1.1+/−.3	1.0+/−.4	.9+/−.2	1.9+/−.6	.9+/−.4
Orientation of Mode y	20°N of E	32°S of E	10°S of E	38°N of E	30°N of E
Mode y Natural Frequency Est. (Hz)	.327	.328	.327	.327	.323
y Mode Total Damping Ratio Est.	1.3+/−.3	1.4+/−.4	1.1+/−.3	1.9+/−.7	1.5+/−.5

*Dynamic Absorber was operating during this reel. See OTC 4283

TABLE 2

DAMPING SUMMARY

MODAL DAMPING RATIO ESTIMATES (%)	Reel 1, 3/24/80		Reel 3, 3/25/80		Reel 4, 3/28/80	
	Mode x	Mode y	Mode x	Mode y	Mode x	Mode y
1. ξ_T – Total Measured	1.1+/−.3	1.3+/−.3	1.0+/−.4	1.4+/−.4	.9+/−.2	1.1+/−.3
2. ξ_{ST} – Steel Hysteretic	0.24	0.24	0.24	0.24	0.24	0.24
3. ξ_{RAD} – Radiation	0.11	0.11	0.11	0.11	0.11	0.11
4. ξ_{VH} – Viscous Hydrodynamic	0.11	0.11	0.17	0.17	0.14	0.14
5. $\xi_T - (\xi_{RAD} + \xi_{VH} + \xi_{ST})$	.64	.84	.48	.88	.41	.61
6. ξ_{SOIL} for $\xi_{smd} = 0.03$	0.53	0.53	0.53	0.53	0.53	0.53
7. ξ_{SOIL} for $\xi_{smd} = 0.05$	0.88	0.88	0.88	0.88	0.88	0.88

TABLE 3

COMPARISON OF PREDICTED AND MEASURED
HELIDECK ACCELERATION RESPONSES

	REEL 3	REEL 4
Date Recorded	3/25/80	3/28/80
Natural frequency f_x (Hz)	.323	.323
$G_\eta(f_x)$ (ft^2/Hz)	1.2	.7
$\xi_{RAD}(f_x)$ (%)	.11	.11
$\xi_T(f_x)$ (%)	1.0+/-.4	.9+/-.2
ξ_{RAD}/ξ_T	.110	.122
σ_{ap}^2 (ft^2/sec^4) (95% confidence bounds)	1.09 (.78 to 1.82)	.71 (.58 to .91)
σ_{am}^2 (ft^2/sec^4)	.91	.72

M = 3162 lb-sec^2/ft, (slugs), modal mass

ρ_w = 1.988 lb-sec^2/ft^4 (slugs/ft^3)

g = 32.11 ft/sec^2

σ_{ap}^2 = total predicted mean square helideck displacement
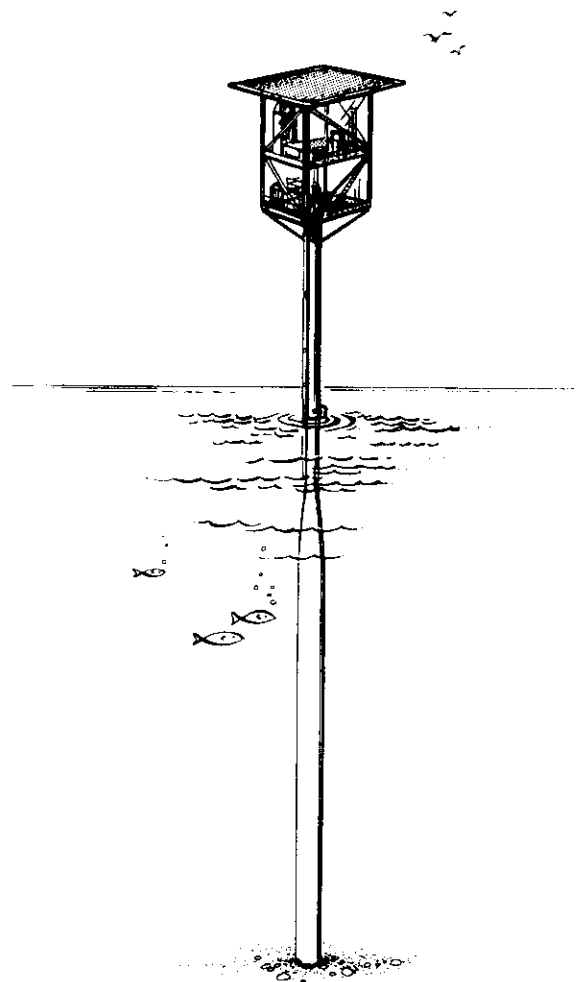
σ_{am}^2 = total measured mean square helideck displacement

Fig. 1 — Caisson production platform

Fig. 2 — Coordinate system definition

Fig. 3 — Finite element model